Title: Membrane potential modulates ERK activity and cell proliferation

Authors: Mari Sasaki[1]*, Masanobu Nakahara[1], Takuya Hashiguchi [1], Fumihito Ono [1],

Affiliations:

[1] Department of Physiology, Division of Life Science, Faculty of Medicine, Osaka Medical and Pharmaceutical University; Takatsuki, Osaka, Japan.

*Corresponding author. Email: mari.sasaki@ompu.ac.jp

Summary: The plasma membrane potential has been linked to cell proliferation for more than 40 years. Here we experimentally showed that membrane depolarization upregulates cell mitosis, and that this process is dependent on voltage-dependent activation of ERK. ERK activity exhibits a membrane potential-dependency that is independent from the growth factor. This membrane potential dependence was observed even close to the resting membrane potential, indicating that small changes in resting membrane potential can alter cell proliferative activity. The voltage-dependent ERK activity is derived from changed dynamics of phosphatidylserine which is present in the plasma membrane and not by extracellular calcium entry. The data suggests that crucial biological processes such as cell proliferation are regulated by the physicochemical properties of the lipid. This study suggests that membrane potential may have diverse physiological functions beyond the action potential, which is well-established in the neural system.

Introduction:

The plasma membrane potential is the voltage difference across the bilayer membrane of a cell that is established by the balance of intracellular and extracellular ion concentrations and their conductance. Intracellular and extracellular ion concentrations are maintained by passive and active ion transport through various ion channels and transporters located in the membrane. While individual cells have distinct resting plasma membrane potentials, the physiological function of membrane potential has been discussed mainly in excitable cells, i.e. muscle and nerve, and non-excitable cells have received less attention (1, 2).

However, accumulating evidence suggests that the physiological importance of membrane potential is not limited to the action potential in the excitable cells (3). Membrane potential has been suggested to be involved in pattern formation in early embryogenesis, regeneration and cancer (4). For example, membrane potential is a determinant factor for the left-right patterning in early embryogenesis (5). It is also known that resting membrane potential is related to proliferative capacity (6-10). These studies showed that depolarized cells have a higher level of mitotic activity. Moreover, Voorhess et al. reported that sustained depolarization induced DNA synthesis in chick spinal cord neurons (11). These results are consistent with the observation that oncogenetically transformed cells are generally more depolarized than normal parental cells (12). Although there have been many reports indicating that membrane potential regulates cell proliferation, the molecular mechanisms by which membrane potential regulates cell proliferation have not been investigated in parallel.

Cell proliferation is regulated by various growth factors and downstream intracellular signaling cascades such as mitogen-activated protein kinase (MAPK) cascades. Extracellular signal-regulated kinase (ERK) is one of the key molecules that regulate cell proliferation (13). The ERK

signaling pathway is often upregulated in human tumors. In contrast, when cells become confluent and proliferative activity becomes slow, ERK activity is downregulated (14).

Zhou et al. reported that phosphatidylserine and K-Ras appear to undergo a change in their nanoscale organization upon plasma membrane depolarization (15). Zhou et al. also demonstrated that voltage-dependent ERK activation occurs when constitutive active K-RasG12V mutant are overexpressed. However, cell proliferative capacity was not the main focus of this paper. It still remains unclear whether voltage-dependent ERK can explain the membrane potential-dependent cell proliferative capacity.

Here, we show experimental evidence that depolarization does induce mitosis, which is associated with the activation of ERK.

Result

Mitotic activity is upregulated by membrane depolarization via MAPK cascade

Cell proliferation has been linked to membrane voltage for decades (9). We first investigated whether there is a causal relationship between membrane potential and mitotic activity in our experimental system. To focus on the mitotic phase of the cell cycle, U2OS cells were synchronized at the G1 phase by treating them with 2 mM thymidine for 20 hours, followed by 8-9 hours of normal incubation (G1 release). The cells were subsequently time-lapse imaged. Cytokinesis, which was easily recognized by brightfield images (Fig.1A), was counted for each frame. The number of cells in the mitotic phase was increased 12-13 hours after G1 release, which corresponds to 4 hours after the start of time-lapse imaging (Fig1B.). The mitotic activity, defined by the number of cells that have undergone cell division, was significantly upregulated in cells treated with a 15 mM high K^+ solution (Fig.1B and C). This result indicates that membrane depolarization induce mitotic activity, which means there is a causal relationship between membrane potential and mitotic activity.

We next investigated the potential involvement of ERK in the depolarization-induced mitotic activity. When cells were treated with MEK inhibitor (U0126), the effect of 15mM high K^+ solution-induced mitotic activation was abolished, indicating that MEK activation play a pivotal role in depolarization induced proliferation (Fig.1B and C).

These result indicated that MEK-ERK activation was involved in the depolarization-induced mitotic activation. However, our results were not consistent with those of a previous report, which indicated that ERK is only activated when the extracellular potassium concentration is above 50 mM in cells expressing wild-type K-Ras (15). Therefore, it remains unclear whether the depolarization-induced mitotic activation could be explained by voltage-dependent activation of ERK. We therefore investigated whether ERK is activated by physiological range of membrane depolarization.

ERK activity has voltage-dependency with the physiological rang of membrane potential

While Western blot is an excellent method for studying all-or-nothing phenomena, it is not well-suited for quantitatively capturing small changes or capturing phenomena with large cell to cell variability. Furthermore, it is not an appropriate method for studying detailed kinetics. To address these limitations, live cell imaging was used in this study. ERK activity was monitored by the Förster Resonance Energy Transfer (FRET) imaging using an ERK biosensor called EKAREV

while the plasma membrane potentials were manipulated by changing the extracellular potassium concentration. EKAREV is the intramolecular FRET biosensor which changes its conformation depending on the ERK activity (16). Ypet and ECFP were used as the FRET pair, which we will refer to as YFP and CFP, respectively, for simplicity.

When U2OS cells expressing EKAREV were perfused with 145 mM high K^+ solution, the YFP/CFP ratio increased over the next 10-20 min, indicating that ERK activity was upregulated (Fig.2A, B). This kinetics is consistent with previous report (15). We confirmed that our experimental system could capture depolarizing-induced ERK activation.

For quantitative analysis, two types of normalization were combined in order to facilitate the detection of small differences. One is to normalize the variation among dishes and the other is to normalize the variation among cells. Since the raw YFP/CFP value varied among dishes, presumably due to the difference in the expression level of the EKAREV probe and the background noise, the YFP/CFP value before application of the high K^+ solution was averaged and used as a reference. The ratio of the raw YFP/CFP value to the reference value was defined as the normalized YFP/CFP value. The other is to normalize the variation among cells. they were stimulated with EGF (10 ng/mL) to strongly activate ERK activity, which was used as the maximum ERK activity for each cell. We defined the % ERK activity as the high K^+-induced ERK activity (relative to the reference) divided by the maximum activity with EGF stimulation. These quantitative analyses were performed on imaged single cells (Fig.2B-F).

ERK activity was upregulated by perfusion with 145 mM high K^+ solution (Fig. 2A and B). We observed similar results in HEK293 cells, HeLa cells and A431 cells (fig.S1). The mean ERK activity with 145 mM high K^+ perfusion was unexpectedly close to 100% (Fig.2B), indicating that depolarization induced by 145 mM K^+ has a similar impact on cells as EGF stimulation. Since extracellular 145 mM high K^+ solution is distant from a physiological condition, we next examined the 30 mM K^+ perfusion, which did not result in ERK activation in the previous report (15). By using our imaging-based experimental system, we were able to detect ERK activation with 30 mM K^+ perfusion. We could detect ERK activation even with 15 mM K^+ perfusion where we observed mitotic upregulation, which means even a small depolarization within the physiological range could activate ERK, which in turn promotes cell division. Of note, U2OS cells expressed wild-type K-Ras but not an active mutant of K-Ras, which means voltage-dependent ERK activation occurs not only in tumor cells but also in normal cells. The average ERK activity with 30 mM K^+ perfusion was about half of the maximum. The average ERK activity was further reduced when perfused with the 15 mM K^+ solution (Fig.2B). These results indicated that ERK has voltage dependent activity not only at high membrane potential (depolarization) but also in a range close to the resting membrane potential. This is an observation that differs from previous studies (15).

Another advantage of our imaging-based experimental system is that we could quantify the ERK activity in each cell. When individual cells were examined for the responses, the overall distribution was not Gaussian and a large proportion of cells perfused with 145 mM K^+ solution showed % ERK activity of 90% or higher (Fig. 2C and D). On the other hand, % ERK activity of cells perfused with 30 mM high K^+ solution was concentrated around 50 ~ 60%, and the averaged response was lower. The variance of the response was larger in cells perfused with 15 mM high K^+, with a significant proportion of cells showing no response (Fig. 2C and D).

The correlation coefficient between the % ERK activity and the logarithm of the extracellular K^+ concentration was 0.54 (Fig.2D). Since the membrane potential is proportional to the logarithm of the extracellular K^+ concentration based on the Nernst equation, these data indicated that ERK

activity was voltage dependent not only at high membrane potentials but also in the physiological range of membrane potentials.

ERK is activated by various growth factors as well as by various stimuli such as neural excitation or mechanosensory input (17, 18), where the extracellular source of calcium entry is occasionally implicated. ERK activation in neurons was abolished when extracellular calcium was depleted (19). Calcium entry is also important in mechanosensory input. Mechanical stretch induces the opening of the stretch-activated Piezo1 channel and the calcium influx. We therefore tested whether extracellular calcium entry is involved in voltage-dependent ERK activation.

When cells were perfused with calcium-free145 mM K^+ solution, ERK was activated to the same extent as the EGF stimulation, suggesting that calcium entry from the extracellular space is not necessary for voltage-dependent activation of ERK (Fig.2E and F).

ERK activity depends on plasma membrane potential

ERK was only activated above -10mV with wild-type K-Ras in the previous study (15). In order to gain further insight into the relationship between voltage-dependent ERK activation and absolute membrane potential, we employed electrophysiology as a research tool.

ERK activity was monitored by EKAREV FRET imaging, while depolarization was achieved by the voltage clamping. Since U2OS cells were not amenable to the giga-seal formation required for patch clamping, we instead used HEK293 cells stably expressing the ERK biosensor EKAREV.

In a preliminary experiment, we performed the whole-cell configuration but failed to observe ERK activation even with EGF stimulation, suggesting that the intracellular component necessary for ERK activation was depleted by the whole-cell configuration. Thus, we next turned to the perforated patch-clamp technique using gramicidine (called perforated patch clamp), which keeps the intracellular component intact while allowing ions to pass through membrane pores.

HEK293 cells stably expressing EKAREV were depolarized from a holding potential of -80 mV. A control cell in the same optical view, whose membrane voltage was not manipulated, is shown in blue (Fig. 3A-F).

Depolarization to -40 mV did not upregulate ERK (Fig.3A and D). Depolarization from -80 mV to -20 mV significantly activated ERK (Fig. 3B and 3E). Depolarization to 0 mV caused the strongest activation of ERK, close to the maximum level (Fig. 3C and F).

In our experimental condition, HEK cells exhibited resting membrane potential ranging from -36 mV to -15 mV. This is in line with the lack of ERK activation at -40 mV.

Again we showed voltage-dependent ERK activation within the membrane potential range which was not observed in the previous study (15).

Notably, ERK activity was reduced with a fast time course (within 1 minute) after repolarization to -80 mV, which was much faster kinetics than the previous report of 30 min (15). Faithful and swift change of the ERK activity coupled to the membrane potential is in contrast to its activation caused by EGF, which does not decline for more than 10 minutes (Fig. 3B, 3C,3E and 3F).

The correlation coefficient between % ERK activity and membrane potential was 0.54 (Fig.3G), again suggesting that ERK activity is voltage dependent even when close to the resting membrane potential. We also confirmed that depolarization (0 mV) alone was sufficient to activate ERK to a level comparable (88±35%) to the EGF stimulation (Fig. 3G).

The variance of % ERK activity was larger with the depolarization pulse at -20mV compared to 0 mV or -40mV (Fig.3G). We speculate that it is due to the range of resting membrane potentials we observed, between -36 mV to -15 mV: i.e. the polarity of the voltage changes from the resting potential to -20 mV is expected to be different in individual cells, which determined the ERK activation.

MAPK cascade was activated upon depolarization

We confirmed ERK activation upon high K^+ perfusion by Western blot. 145 mM high K^+ perfusion was used in this experiment, because 50 mM high K^+ did not upregulate ERK activity with Western blot (15). U2OS cells were perfused with 145 mM high K^+ solution and subsequently lysed with lysis buffer. ERK was indeed phosphorylated upon high K^+ perfusion (Fig.4A and B).

We next examined the involvement of upstream molecules implicated in the ERK signaling cascade, namely the MAPK cascade with same condition (145 mM K^+). MEK and c-Raf, located upstream of ERK in the canonical pathway, were also phosphorylated by the 145 mM high K^+ perfusion (Fig. 4A and 4B). These results indicated that the MAPK cascade had a depolarization-activated pathway.

Our real-time imaging data revealed that depolarization-induced ERK activation has considerably slower kinetics than voltage-dependent ion channels, which typically activate within a millisecond (20). We next examined the kinetics of the upstream pathway of MAPKs with imaging-based methods so that detail kinetics can be monitored.

Ras was activated upon depolarization with fast kinetics

We examined Ras activity, which is upstream of c-Raf. Although nonoclusters of Ras were known to cause activation of downstream MAPK cascade, there were no direct data to date on whether Ras is activated by depolarization. Ras activity was monitored by imaging with a FRET-based biosensor called Raichu-Ras (21). Raichu-Ras is an intramolecular FRET biosensor which changes its conformation and triggers an increase in FRET depending on the Ras activity. The lifetime of the donor becomes shorter when FRET occurs. We aimed to monitor Ras activity in an area restricted to the vicinity of the plasma membrane. Ras activity was monitored by fluorescence lifetime imaging microscopy combined with fluorescence resonance energy transfer (FLIM-FRET) (21). U2OS cells expressing Raichu-Ras were perfused with 145mM high K^+ solution followed by perfusion with EGF solution (10ng/mL).

The mean fluorescence lifetime of the donor fluorophore of Raichu-Ras on the plasma membrane decreased within 2 minutes after 145mM K^+ perfusion, indicating the Ras activation (Fig. 4C). The activation kinetics were similar between high K^+ stimulation and EGF stimulation, which was much faster than depolarization-induced ERK activation. The time course of activation was also consistent with the previous report (15, 22). This data suggested that Ras was activated by membrane depolarization with faster kinetics than that of ERK.

The phosphatidylserine dynamics was involved in the voltage-dependent ERK activity

We further investigated upstream of Ras. Change of membrane potential is expected to be complete within milliseconds, and kinetics upstream of Ras are expected to be at least as fast as that of Ras. Zhou et al. reported that plasma membrane depolarization induces nanoscale reorganization of phosphatidylserine (15). K-Ras, which is targeted to the plasma membrane by

electrostatic interactions with phosphatidylserine, in turn undergoes nanoclustering and amplifies MAPK signaling in fibroblasts, excitable neuroblastoma cells, and Drosophila neurons (15). Based on these findings, we examined the involvement of phosphatidylserine nanoclustering in the voltage-dependent activation of ERK in U2OS cells.

Phosphatidylserine dynamics were monitored by intermolecular FRET using the phosphatidylserine-specific probe LactC2 (Fig.4D). The C2 domain of Lactadherin (LactC2), which binds phosphatidylserine, allows the visualization of phosphatidylserine when conjugated with CFP or YFP (23). The fluorescence lifetime of CFP-LactC2 was 2.375±0.014 ns, which decreased to 2.345±0.013 ns when YFP-LactC2 was co-expressed in the same cells (Fig. 4E), indicating that phosphatidylserine nanoclustering could be monitored by FLIM-FRET. The fluorescence lifetime of CFP-LactC2 in the cells co-expressing the FRET acceptor YFP-LactC2 decreased within 2 minutes upon 145mM high K^+ perfusion, indicating the depolarization-induced nanoclustering of phosphatidylserine (Fig. FC, 4G). The kinetics of depolarization-induced nanoclustering of phosphatidylserine is similar to that of Ras activation, which is a reasonable result if phosphatidylserine and Ras interact.

To confirm that phosphatidylserine dynamics were involved in voltage-dependent ERK activation, phosphatidylserine was depleted by treating cells with fendiline for 48 hours (24). When U2OS cells were treated with fendiline for 36 to 48 hours, high K^+-induced ERK activation was diminished (Fig. 4H and 4I). These results indicate that membrane phosphatidylserine dynamics play a critical role in voltage-dependent ERK activation in U2OS.

Discussion

The relationship between cell proliferation and membrane potential has been discussed since the 1970s. However, the lack of studies that addressed the molecular mechanisms has left the full picture of the relationship between membrane potential and cell proliferative potential unclear. With regards to the molecular mechanisms involved, a study published in 2015 demonstrated a correlation between MAP kinases activity and membrane potential. However, the voltage-dependence of ERK activity has not been demonstrated within the physiological membrane potential range. Therefore, it remains unclear whether voltage-dependent MAP kinase activation can explain the link between membrane potential and cell proliferation. In this study we were able to experimentally demonstrate a causal relationship between membrane potential and mitotic activity (cytokinesis) near the physiological membrane potential, which was associated with depolarization-induced ERK activation via phosphatidylserine dynamics. We were able to connect and clarify the molecular mechanism of the phenomenon that has long been suggested as a correlation between membrane potential and cell proliferative capacity.

We showed membrane depolarization induces mitotic activity through the activation of ERK (Fig.1), which indicates that membrane potential and cell proliferation are not merely correlated but membrane potential itself regulates mitotic activity. Some reports indicated that ERK plays an important role in the S phase entry (25), while other reports proposed that ERK plays a role in mitosis (26-28). Further studies will be needed to elucidate which step of the cell cycle is regulated by membrane potential.

We showed direct evidence that membrane potential itself regulates ERK activity by controlling membrane potential using voltage-clamp to exclude any possibility that factors other than membrane potential regulate ERK activity. Another advantage of electrophysiology is the ability to study the effect of repolarization. With conventional techniques of perfusion it is difficult to change solution instantaneously, which hinders investigating the effect of repolarization.

The characteristics of the ERK response to voltage compared to EGF stimulation was the linearity of the stimulus and the response (Fig2 and 3). It is notable that ERK activity was downregulated with membrane repolarization, while ERK remains active for at least 5 minutes after the growth factor binds to its receptor (29). This implies that membrane potential can act as a fine tuner of ERK, in contrast to the growth factor stimulation acting as an on/off switch.

The imaging analysis using FRET-based probes allowed us to study kinetics for each step of signal transduction e.g. nanoclustering of phosphatidylserine and subsequent activation of Ras was completed within 2 minutes (Fig.4C, 4F), whereas activation of ERK took more than 5 minutes (Fig.2B). This result is reasonable since several molecules have to be activated before ERK activation.

Another advantage of imaging-based analysis is that it allowed us to quantitatively measure ERK activity in individual cells. The variability of the response to depolarization among analyzed cells was surprisingly large. Of note, this variance is averaged and not observable in Western blot analysis, which is routinely used to study intracellular signaling pathways, including ERK. Surprisingly, 0 mV depolarization activated ERK to the same extent as EGF stimulation.

Furthermore, coupled with electrophysiology, we could control and monitor the activity with a time resolution that cannot be achieved by perfusion or biochemical analysis. It revealed that ERK began to activate within 1 minute upon depolarization and sustained activity increase for at least 5 minutes. The kinetics of the deactivation upon repolarization was similar to that of activation.

We also demonstrated that ERK exhibits voltage-dependent behavior, ranging from the resting membrane potential to a high membrane potential (depolarization). This is reasonable when considering that voltage-dependent ERK activation is derived from voltage-dependent phosphatidylserine dynamics on the plasma membrane, which is supposed to be a physiochemical phenomenon. The plasma membrane potential is a novel member of the ERK regulator.

Zhou et al. reported that phosphatidylserine and PIP_2 change their nanoscale organization upon plasma membrane depolarization (15). K-Ras also changes its nanoscale organization based on electrostatic interaction between its basic amino acid residues and anionic phosphatidylserine (15, 30). Such electrostatic interaction may occur between a cluster of basic amino acids in another protein and an anionic phospholipid, i.e. phosphatidylserine or PIP_2. For example, it is known that a cluster of basic amino acids in EGFR interacts with PIP_2 and that EGFR is activated when clustered (31, 32). This suggests that EGFR activity may also be regulated by membrane potential. There are many other proteins which interact with PIP_2 and possess a cluster of basic amino acids, suggesting that membrane potential may regulate the activity of many more proteins than previously thought, and thereby regulate many physiological phenomena.

We showed that membrane potential modulates phosphatidylserine dynamics (Fig.4F amd G). The relationship between the electrostatic potential and the organization of the cell membrane was previously discussed (33). The transmembrane potential affects the lateral sorting of membrane components as well as the positioning of polar lipid headgroups (33). In addition, lipid viscosity, which is influenced by lipid and protein composition and their organization in the membrane, is

altered by the membrane potential (34-36). However, the exact mechanism by which the transmembrane potential can modulate the organization of lipids and proteins in the membrane remains unknown.

Overall, our results link three elements: i.e, the plasma membrane voltage, ERK activity and the cell proliferation, and propose a new signaling cascade regulating cell division. This result provides rationale that ion channels and ion transporters, which regulate the plasma membrane potential, are potential targets for tumor treatment. Moreover, given that ERK is involved also in cell differentiation, migration, senescence and apoptosis (37), membrane potential may also regulate them and prove to be potential targets for future drug developments.

What is the biological meaning of membrane potential regulating cell proliferation ? The stochastic ERK activation reported by Aoki et al. may result from the fluctuation of the membrane potential (38). Furthermore, cell-to-cell propagation of the membrane potential through gap junctions may result in spreading of the ERK activity and synchronized cell proliferation (38). This type of synchronized proliferation could be beneficial in tissue such as epithelium. Our finding that the plasma membrane potential is an analog modulator of ERK activity is consistent with this hypothesis, which would allow nuanced regulation of cell proliferation.

It is now evident that the physiological significance of membrane potential extends beyond its role in ion channels. Given that membrane potential is a physical phenomenon that affects all cellular components, including proteins and lipids, new biological phenomena regulated by membrane potential may exist.

Acknowledgments:

We thank Dr. Michiyuki Matsuda (Kyoto University) for providing us EKAREV and RaichuEV-HRas plasmids. We thank Dr. Michiyuki Matsuda, Dr. Tohru Ishitani and Dr. Jianmin Cui for critical reading of the manuscript. **Funding:** KAKENHI 20K07268 to M.S. Naito Foundation to M.S. Takeda Science Foundation to M.S.

Author contributions:

Conceptualization: MS
Data curation: MS
Formal analysis: MS,MN
Funding acquisition: MS
Investigation: MS, TH
Methodology: MS
Project administration: MS
Software: MS, MN
Writing—original draft: MS
Writing—review & editing: MS, FO

Declaration of interests: The authors declare no competing interests.

Material and Methods

Plasmid and reagents

The expression vectors for EKAREV and Raichu-Ras plasmid were kindly provided by Dr. Michiyuki Matsuda (Kyoto University). mRFP-Lact-C2 was a gift from Sergio Grinstein (Addgene plasmid # 74061 ; http://n2t.net/addgene:74061 ; RRID:Addgene_74061)(23). YFP-LactC2 and CFP-LactC2 plasmids were generated from mRFP-LactC2 plasmid by exchanging mRFP to YPet and SECFP, respectively. Recombinant human EGF was purchased from ThermoFisher Scientific. Fendiline was purchased from CAYMAN Chemical. Gramicidin was purchased from Sigma-Aldrich.

Cells

U2OS cells were purchased from ECACC（European Collection of Authenticated Cell Culture）. U2OS cells were maintained in McCoy's 5A medium supplemented with 10 % fetal bovine serum. HEK293 cells stably expressing EKAREV were generated by PiggyBac transposon system transfection with EKAREV/pPBbsr2 and mPBase/pCMV vectors and were maintained in DMEM medium supplemented with 10 % fetal bovine serum. Cells were cultured in a 5% CO_2-humidified environment at 37°C.

Time-lapse imaging with high K^+ perfusion

U2OS cells were plated on the glass-based dish (Matsunami) and transfected with the EKAREV plasmid using TransIT-LT1 reagent (Mirus) according to the manufacture's instructions. Cells were serum starved for 3 to 16 h before starting the time-lapse FRET imaging. Cells were imaged using an inverted microscope (Ti2-E; Nikon) equipped with a 60× objective (NA=1.4; Nikon), a CMOS camera (Zyla4.2; Andor), and an LED illumination system (xCite Xylis; Excelitas technologies). A W-VIEW GEMINI image splitting system (Hamamatsu Photonics) was used to acquire CFP and YFP images simultaneously. The following filters and dichroic mirrors were used: 439/24 for excitation, 483/32 (CFP) and 542/27 (YFP) for emission, and FF509-fDi01 for the dichroic mirror. FLIM-FRET images were acquired with a Stellaris (Leica) confocal microscope excited at 448 nm. The fluorescence lifetime of the donor fluorophore was measured at 460-500 nm with a pinhole size of 1 A.U. so that only signal from the plasma membrane was detected. The perfusion solution was changed using the valve-controlled gravity perfusion system (VC3-4PG) controlled by Arduino. The solutions were as follows (in mM), 5K ; 140 NaCl, 5 KCl, 1 $CaCl_2$, 1 $MgCl_2$. 15K ; 130 NaCl, 15 KCl, 1 $CaCl_2$, 1 $MgCl_2$. 30K ; 115 NaCl, 30 KCl, 1 $CaCl_2$, 1 $MgCl_2$. 145K ; 145 KCl, 1 $CaCl_2$, 1 $MgCl_2$. 5K (Ca free) ; 140 NaCl, 5 KCl, 1 EGTA, 1 $MgCl_2$. 145K (Ca free) ; 145 KCl, 1 EGTA 1 $MgCl_2$. All solutions contained 20 mM HEPES pH=7.4. EGF solution was prepared with low K^+ solution (5 mM K^+).

Patch clamping

HEK293 cells stably expressing EKAREV were plated on the glass-based dish (Matsunami) and serum starved for 16 hours before starting the experiment. The gramicidin-perforated patch clamp experiment was performed using a Multiclamp700B amplifier and Digidata 1440A and pClamp software (Axon). 60 μg/mL gramicidin in patch solution (145 mM KCl, 5 mM EGTA, 10 mM HEPES pH7.4) was sonicated for 5 minutes and back-filled to the patch pipette. 5K solution was used as external patch solution. FRET images were acquired with a confocal microscope LSM510Meta (Ziess) excited at 458 nm. The filters used for CFP and YFP were 475-525 and LP530, respectively.

Imaging Analysis

The dead cells and unhealthy cells that did not respond to EGF stimulation were excluded from the analysis. The average intensity of the multiple background ROIs was used as the background and subtracted from each image. The fluorescence intensities of the YFP channel and CFP channel were averaged for each cell, and the results were exported as a CSV file. The YFP/CFP value was calculated using Excel and R Studio for the patch-clamp and high-K^+ perfusion experiments, respectively. The % ERK activity was calculated by dividing the maximum normalized YFP/CFP ratio after high K^+ perfusion or depolarization by the maximum normalized YFP/CFP ratio after EGR perfusion for each cell. For the FLIM-FRET experiment, the average fluorescence lifetime was calculated for each cell. The fluorescence lifetime of the first 10 minutes was averaged and used as a reference. The ratio of fluorescence lifetime to the reference value was defined as normalized fluorescence lifetime. All image analysis was performed using ImageJ software.

Western blot

The following antibodies were used for Western blotting: total ERK (SantaCruz, SC514302); phospho-ERK (CST, 4370); total MEK (CST, 4394); phospho-MEK (CST, 2338); total c-Raf (CST, 9422); phospho-c-Raf (CST9431). Cells were lysed in 50 mM Tris (pH 7.5), 150 mM NaCl, 1 mM EDTA, 1% NP40 with protease and phosphatase inhibitor cocktail (Thermo Scientific), 1 mM sodium orthovanadate. Protein samples (10 mg per lane) were separated by SDS-PAGE electrophoresis and immunoblotted on polyvinylidene fluoride (PVDF) membranes and detected by ECL using a charge-coupled device (CCD) camera. Quantification was performed using ImageJ software.

Mitosis analysis

U2OS cells were synchronized at the G1 phase by treating them with 2 mM thymidine for 20 hours. Time-lapse imaging was conducted after 8~9 hours following G1 release using an inverted confocal microscope (Stellaris; Leica) with a 20× objective (NA=0.75) using DIC mode. The images were taken in solution with different K+ concentration (see 'Time-lapse imaging with high K^+ perfusion' section for solution composition.) every 10 minute. The number of mitotic cells was counted for each frame.

Statistical Analysis

Statistical analysis was performed using R studio. The level of statistical significance is indicated by asterisks: ns $p > 0.05$, * $p < 0.05$, ** $p < 0.01$, *** $p < 0.001$, **** $p < 0.0001$.

Fig.1 Mitotic activity is upregulated by membrane depolarization.

(A) Representative image of mitotic cell. The images were 20 minute before and after cytokinesis. Scale bar is 10 μm. (B) The number of mitotic cells was accumulated for every 1.5 hours and normalized against those of first 1.5 hour with 5 K solution and plotted against time after starting the time-lapse imaging. Data are mean±SEM (C) Accumulated total mitotic cell number for 7.5 hours. p=0.044 (one sample t-test). U; U0126

Fig.2 ERK is activated upon high K+ perfusion.

(A) YFP/CFP ratio images at the indicated time points. Serum starved U2OS cells expressing EKAREV were perfused with 145 mM high K+ solution at 10 minutes, followed by the addition of 10 nM EGF at 30 minutes. Scale bar is 10 mm. The color scale indicates YFP/CFP ratio. (B) ERK activity with high K+ perfusion. Serum-starved cells were treated with various concentrations of K+ solution at 10 min, followed by the addition of 10 nM EGF at 30 min. Normalized % ERK (response by high K / response by EGF; see in the text) activity was calculated as follows, the normalized YFP/CFP (see in the text) was divided by the normalized maximum YFP/CFP after subtracting the mean normalized YFP/CFP at 8-10 min. Data are mean±SEM. N=16, 15 and 23 for 145K+, 30K+ and 15K+, respectively. (C) The relationship between the K+ concentration and the % ERK activity. p=0.00013 (Kruskal-Wallis). (D) The relationship between the logarithm of K+ concentration and the % ERK activity. R is Pearson's correlation coefficient. The gray area is 95% confidence interval. (E) Mean normalized YFP/CFP ratio perfused with Ca+ free 145 K+ high K solution. Starved cells were incubated with 5K+ (Ca+ free) solution, followed by perfusion with 145mM K+ (Ca+ free) solution at 10 min. 10nM EGF was added at 30 min. Data are mean±SEM. N=14 (F) The % ERK activity in the Ca(+) and Ca(-) solution. The data for Ca(+) were the same as in Fig.2C(145K+). p=0.82 (Wilcoxon rank sum exact test)

Fig.3 ERK activity depends on membrane voltage

(A to C) Mean normalized YFP/CFP ratio. Starved cells were depolarized from a holding potential of -80mV to depolarized membrane potentials (-40, -20 and 0 mV for A, B, and C, respectively) at 5 minutes, followed by repolarization to -80mV at 10 minute. 10nM EGF was perfused at 15 minutes. Data are mean±SD. N=4, 8 and 10 for -40, -20 and 0 mV, respectively. (D to F) Average normalized YFP/CFP ratio for the first 5 min (-80mV), maximum normalized YFP/CFP ratio at depolarized phase (-40, -20 and 0mV for A, B, and C, respectively), minimum normalized YFP/CFP ratio at repolarized phase (-80mV) and maximum normalized YFP/CFP ratio at EGF stimulated phase (EGF), respectively. Data are mean±SEM. The p-values were calculated using Student’s t test. (G) The relationship between membrane potential and % ERK activity. p=0.0042 (Kruskal-Wallis). R is Pearson's correlation coefficient. The gray area is 95% confidence interval.

Fig.4 The molecular mechanism by which regulate depolarization-induced mitosis.

(A) Immunoblot analysis of cells perfused with 145K+ solution. (B) Quantification of relative mean band intensity of pERK, pMEK and pcRaf from independent experiments conducted as in

(A). Data are mean±SD. (C) Ras activity was monitored by FLIM-FRET imaging. The donor (mTurquoise-GL) lifetime of U2OS cells expressing Raichu-Ras at the indicated time point. The experimental condition was the same as in Fig.2A. Data are mean±SEM. N= 17 (D) Schema of intermolecular FRET experiment. Phosphatidylserine clustering was monitored by FLIM-FRET imaging of U2OS cells co-expressing CFP-LactC2 and YFP-LactC2. (E) The fluorescence lifetime of CFP-LactC2. The fluorescence lifetime of CFP-LactC2 decreased when YFP-LactC2was co-expressed in the same cells. p=0.00080 (Welch Two Sample t-test) (F) The normalized fluorescence lifetime of CFP-LactC2 was measured at the indicated time point. The experimental condition was the same as in Fig.2A except the EGF stimulation. Data are mean±SEM. N=25 (G) CFP-LactC2 lifetime images at the indicated time points. The experimental condition is described above. Scale bar is 10 μm. The color scale indicates CFP-LactC2 lifetime. (H) Mean normalized YFP/CFP ratio from phosphatidylserine-depleted starved cells treated with 145 K+ solution at 10 minute, followed by the addition of 10nM EGF. Data are mean±SEM. N=25 (I) The % ERK activity with or without Fendiline treatment. The data for Fendiline(-) were the same as in Fig.2C(145K+). p=4.4e-9(Wilcoxon rank sum exact test).

References

1. A. L. Hodgkin, A. F. Huxley, The components of membrane conductance in the giant axon of Loligo. *The Journal of Physiology* **116**, 473-473 (1952).
2. E. Neher, B. Sakmann, Single-channel currents recorded from membrane of denervated frog muscle fibres. *Nature 1976 260:5554* **260**, 799-802 (1976).
3. R. N. Khan *et al.*, Emerging Roles of the Membrane Potential: Action Beyond the Action Potential. *Front. Physiol* **9**, 1661-1661 (2018).
4. M. Levin, Bioelectric signaling: Reprogrammable circuits underlying embryogenesis, regeneration, and cancer. *Cell* **184**, 1971-1989 (2021).
5. M. Levin, T. Thorlin, K. R. Robinson, T. Nogi, M. Mercola, Asymmetries in H+/K+-ATPase and cell membrane potentials comprise a very early step in left-right patterning. *Cell* **111**, 77-89 (2002).
6. S. Sundelacruz, M. Levin, D. L. Kaplan, Role of membrane potential in the regulation of cell proliferation and differentiation. *Stem Cell Reviews and Reports* **5**, 231-246 (2009).
7. D. J. Blackiston, K. A. McLaughlin, M. Levin, Bioelectric controls of cell proliferation: Ion channels, membrane voltage and the cell cycle. *Cell Cycle* **8**, 3527-3536 (2009).
8. C. D. Cone, M. Tongier, Contact inhibition of division: Involvement of the electrical transmembrane potential. *Journal of Cellular Physiology* **82**, 373-386 (1973).
9. C. D. Cone, Unified theory on the basic mechanism of normal mitotic control and oncogenesis. *Journal of Theoretical Biology* **30**, 151-181 (1971).
10. R. Binggeli, R. C. Weinstein, Membrane potentials and sodium channels: Hypotheses for growth regulation and cancer formation based on changes in sodium channels and gap junctions. *Journal of Theoretical Biology* **123**, 377-401 (1986).

11. M. L. Voorhess, M. J. Stuart, J. A. Stockman, F. A. Oski, J. Pediatr, Induction of Mitosis in Mature Neurons in Central Nervous System by Sustained Depolarization. *Science* **192**, 155-158 (1976).
12. S. Tokuoka, H. Morioka, The Membrane Potential of the Human Cancer and Related Cells (I). *Gann* **48**, 353-354 (1957).
13. G. Pages *et al.*, Mitogen-activated protein kinases p42mapk and p44mapk are required for fibroblast proliferation (protein kinase cascade/kinase antiense/dominant neptve mutants/growth control/H-killing selection). *Proc. Natl. Acad. Sci. USA* **90**, 8319-8323 (1993).
14. J. Wayne, J. Sielski, A. Rizvi, K. Georges, D. Hutter, ERK regulation upon contact inhibition in fibroblasts. *Molecular and Cellular Biochemistry* **286**, 181-189 (2006).
15. Y. Zhou *et al.*, Membrane potential modulates plasma membrane phospholipid dynamics and K-Ras signaling. *Science* **349**, 873-876 (2015).
16. N. Komatsu *et al.*, Development of an optimized backbone of FRET biosensors for kinases and GTPases. *Molecular Biology of the Cell* **22**, 4647-4656 (2011).
17. C. D. Harvey *et al.*, A genetically encoded fluorescent sensor of ERK activity. *Proceedings of the National Academy of Sciences of the United States of America* **105**, 19264-19269 (2008).
18. F. Crozet, R. Levayer, Emerging roles and mechanisms of ERK pathway mechanosensing. **80**, 355-355 (2023).
19. J. C. Corvol *et al.*, Depolarization activates ERK and proline-rich tyrosine kinase 2 (PYK2) independently in different cellular compartments in hippocampal slices. *Journal of Biological Chemistry* **280**, 660-668 (2005).
20. F. Bezanilla, The voltage sensor in voltage-dependent ion channels. *Physiological Reviews* **80**, 555-592 (2000).
21. N. Mochizuki *et al.*, Spatio-temporal images of growth-factor-induced activation of Ras and Rap1. *Nature 2001 411:6841* **411**, 1065-1068 (2001).
22. H. Murakoshi *et al.*, Single-molecule imaging analysis of Ras activation in living cells. *Proceedings of the National Academy of Sciences of the United States of America* **101**, 7317-7322 (2004).
23. T. C. U. s. D. y. s. p. Yeung *et al.*, Membrane phosphatidylserine regulates surface charge and protein localization. **319**, 210-213 (2008).
24. K.-j. Cho *et al.*, Inhibition of Acid Sphingomyelinase Depletes Cellular Phosphatidylserine and Mislocalizes K-Ras from the Plasma. **36**, 363-374 (2016).
25. J. G. Albeck, G. B. Mills, J. S. Brugge, Frequency-modulated pulses of ERK activity transmit quantitative proliferation signals. *Molecular cell* **49**, 249-261 (2013).
26. P. S. Shapiro *et al.*, Activation of the MKK/ERK pathway during somatic cell mitosis: Direct interactions of active ERK with kinetochores and regulation of the mitotic 3F3/2 phosphoantigen. *Journal of Cell Biology* **142**, 1533-1545 (1998).
27. F. S. Willard, M. F. Crouch, MEK, ERK, and p90RSK are present on mitotic tubulin in Swiss 3T3 cells: A role for the MAP kinase pathway in regulating mitotic exit. *Cellular Signalling* **13**, 653-664 (2001).
28. E. Iwamoto *et al.*, ERK Plays a Role in Chromosome Alignment and Participates in M-Phase

Progression. *Journal of Cellular Biochemistry* **117**, 1340-1351 (2016).

29. A. Kiyatkin, I. K. Van Alderwerelt Van Rosenburgh, D. E. Klein, M. A. Lemmon, Kinetics of receptor tyrosine kinase activation define ERK signaling dynamics. *Sci. Signal* **13**, 5267-5267 (2020).
30. Y. Zhou, J. F. Hancock, Ras nanoclusters: Versatile lipid-based signaling platforms. *Biochimica et biophysica acta* **1853**, 841-849 (2015).
31. Y. Wang *et al.*, Regulation of EGFR nanocluster formation by ionic protein-lipid interaction. *Cell Research* **24**, 959-976 (2014).
32. K. B. A. Halim, H. Koldsø, M. S. P. Sansom, Interactions of the EGFR juxtamembrane domain with PIP2-containing lipid bilayers: Insights from multiscale molecular dynamics simulations. *Biochimica et Biophysica Acta - General Subjects* **1850**, 1017-1025 (2015).
33. J. Malinsky, W. Tanner, M. Opekarova, Transmembrane voltage: Potential to induce lateral microdomains ☆. 10.1016/j.bbalip.2016.02.012 (2016).
34. P. S. O'Shea, S. Feuertstein-Thelen, A. Azzi, Membrane-potential-dependent changes of the lipid microviscosity of mitochondria and phospholipid vesicles. *Biochemical Journal* **220**, 795-801 (1984).
35. P. Herman, J. Malinsky, J. Plasek, J. Vecer, Pseudo Real-Time Method for Monitoring of the Limiting Anisotropy in Membranes. *JOFL] Journal of Fluorescence* **14** (2004).
36. G. Grossmann, M. Opekarová, J. Malinsky, I. Weig-Meckl, W. Tanner, Membrane potential governs lateral segregation of plasma membrane proteins and lipids in yeast. *EMBO Journal* **26**, 1-8 (2007).
37. Y. Sun *et al.*, Signaling pathway of MAPK/ERK in cell proliferation, differentiation, migration, senescence and apoptosis. *Journal of Receptors and Signal Transduction* **35**, 600-604 (2015).
38. K. Aoki *et al.*, Stochastic ERK activation induced by noise and cell-to-cell propagation regulates cell density-dependent proliferation. *Molecular Cell* **52**, 529-540 (2013).

A

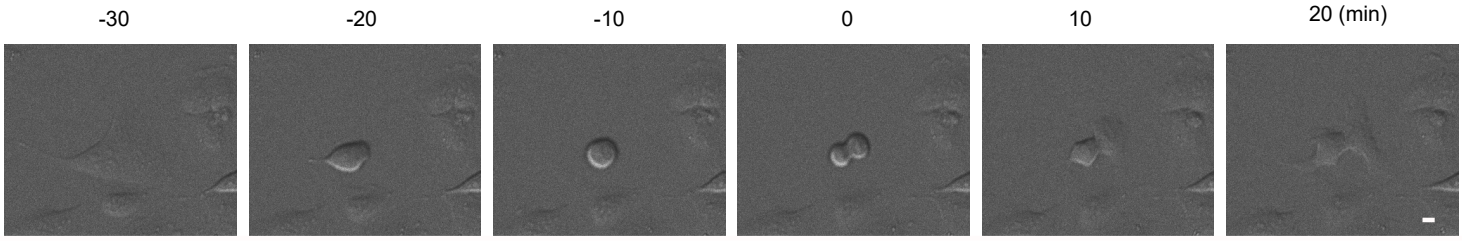
-30
-20
-10
0
10
20 (min)

B

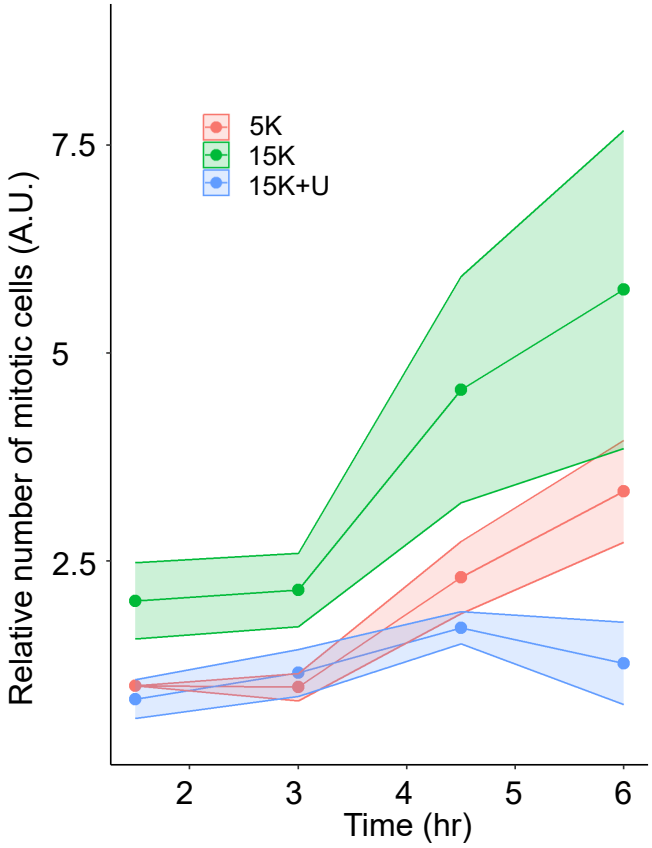
5K
15K
15K+U
Relative number of mitotic cells (A.U.)
7.5
5
2.5
2
3
4
5
6
Time (hr)

C

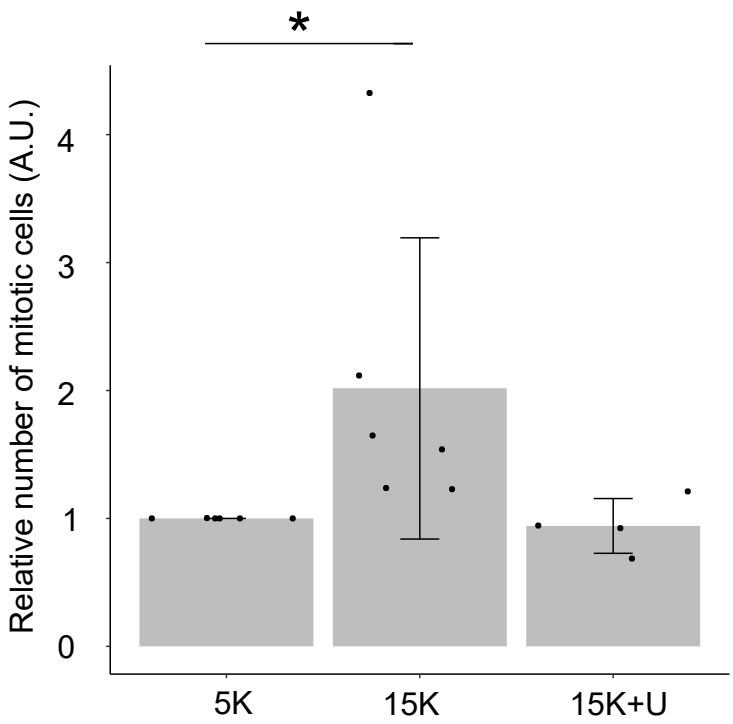
*
Relative number of mitotic cells (A.U.)
4
3
2
1
0
5K
15K
15K+U

Fig1

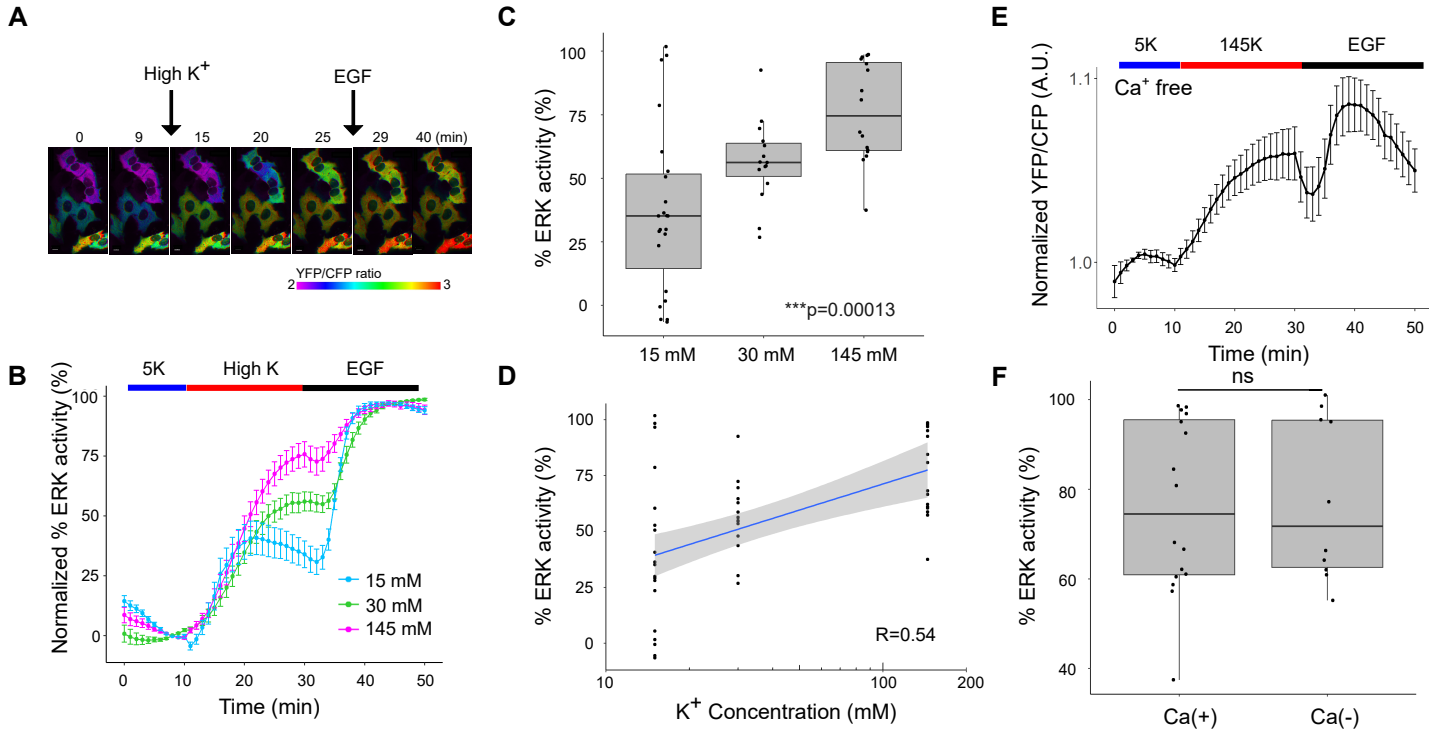
A
High K+
EGF
0
9
15
20
25
29
40 (min)
YFP/CFP ratio
2
3
B
5K
High K
EGF
Normalized % ERK activity (%)
Time (min)
15 mM
30 mM
145 mM
C
% ERK activity (%)
***p=0.00013
15 mM
30 mM
145 mM
D
% ERK activity (%)
R=0.54
K+ Concentration (mM)
E
5K
145K
EGF
Ca+ free
Normalized YFP/CFP (A.U.)
Time (min)
F
ns
% ERK activity (%)
Ca(+)
Ca(-)

Fig.2

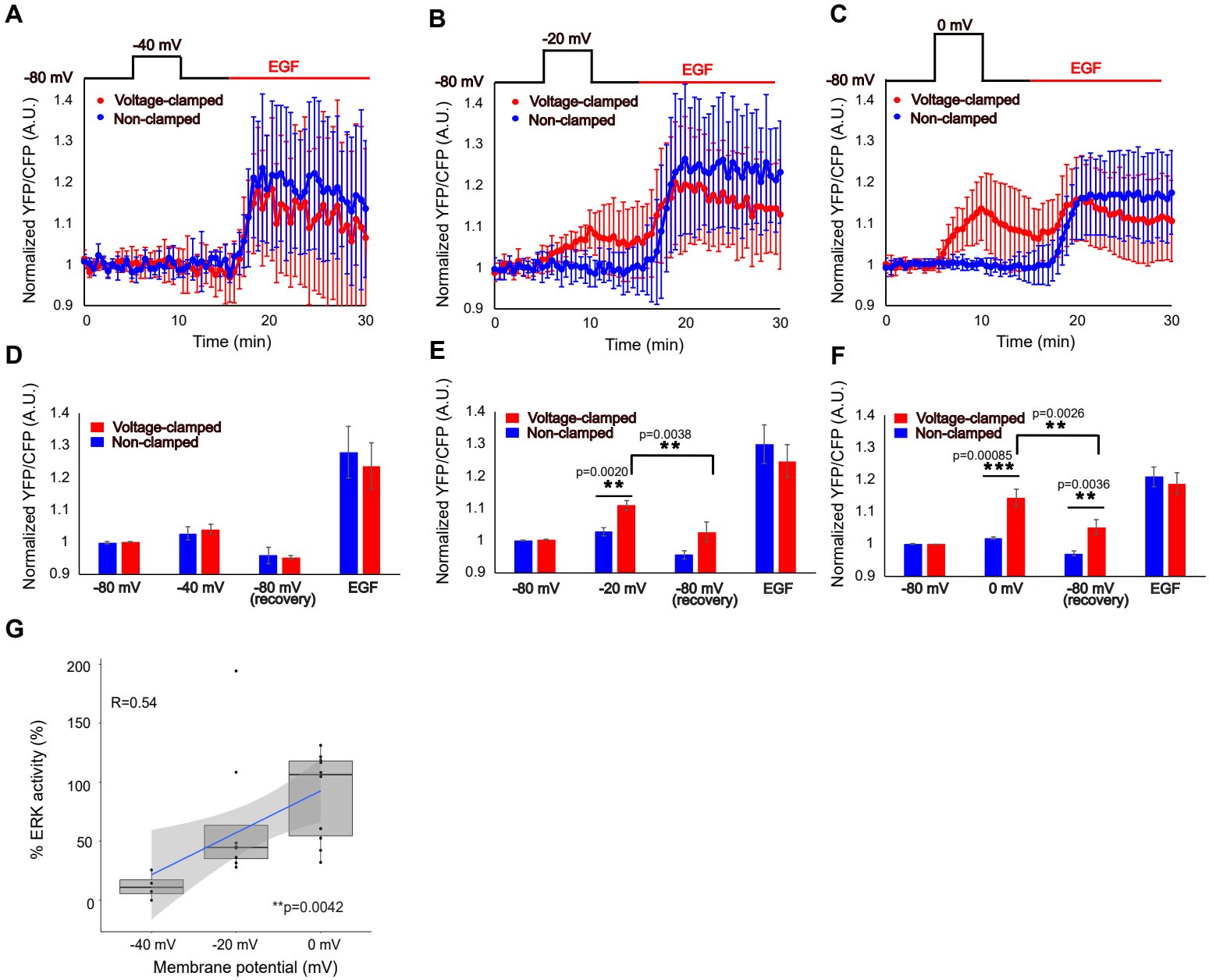
A
-40 mV
-80 mV
EGF
Voltage-clamped
Non-clamped
Normalized YFP/CFP (A.U.)
Time (min)
B
-20 mV
-80 mV
EGF
Voltage-clamped
Non-clamped
Normalized YFP/CFP (A.U.)
Time (min)
C
0 mV
-80 mV
EGF
Voltage-clamped
Non-clamped
Normalized YFP/CFP (A.U.)
Time (min)
D
Voltage-clamped
Non-clamped
Normalized YFP/CFP (A.U.)
-80 mV
-40 mV
-80 mV (recovery)
EGF
E
Voltage-clamped
Non-clamped
p=0.0020
**
p=0.0038
**
Normalized YFP/CFP (A.U.)
-80 mV
-20 mV
-80 mV (recovery)
EGF
F
Voltage-clamped
Non-clamped
p=0.00085
***
p=0.0026
**
p=0.0036
**
Normalized YFP/CFP (A.U.)
-80 mV
0 mV
-80 mV (recovery)
EGF
G
R=0.54
**p=0.0042
% ERK activity (%)
-40 mV
-20 mV
0 mV
Membrane potential (mV)

Fig.3

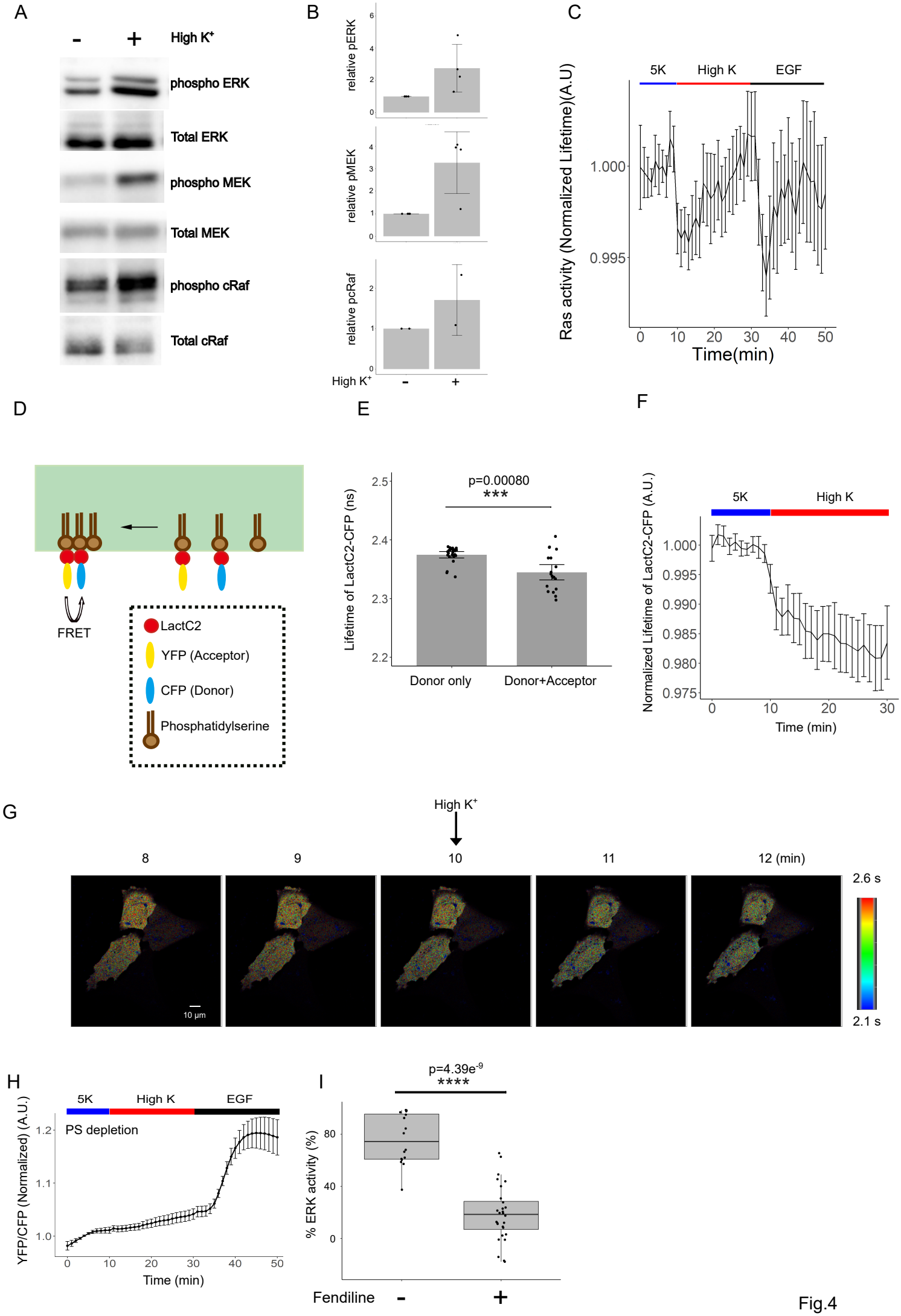
A
-
+
High K+
phospho ERK
Total ERK
phospho MEK
Total MEK
phospho cRaf
Total cRaf
B
relative pERK
relative pMEK
relative pcRaf
High K+
-
+
C
5K
High K
EGF
Ras activity (Normalized Lifetime)(A.U)
1.000
0.995
0
10
20
30
40
50
Time(min)
D
FRET
LactC2
YFP (Acceptor)
CFP (Donor)
Phosphatidylserine
E
p=0.00080
***
Lifetime of LactC2-CFP (ns)
2.5
2.4
2.3
2.2
Donor only
Donor+Acceptor
F
5K
High K
Normalized Lifetime of LactC2-CFP (A.U.)
1.000
0.995
0.990
0.985
0.980
0.975
0
10
20
30
Time (min)
G
High K+
8
9
10
11
12 (min)
2.6 s
2.1 s
10 µm
H
5K
High K
EGF
PS depletion
YFP/CFP (Normalized) (A.U.)
1.2
1.1
1.0
0
10
20
30
40
50
Time (min)
I
p=4.39e-9
****
% ERK activity (%)
80
40
0
Fendiline
-
+

Fig.4